1
On the Track of Reaction Mechanisms: Characterization and Reactivity of Metal Atom Dimers

Hans-Jörg Himmel

1.1
Introduction

The matrix-isolation technique is now well established as a valuable method to retain and characterize reaction intermediates [1]. In this chapter, it will be shown how this method can be used to characterize metal atom dimers and to shed light on their special reactivity. An understanding of the bond properties and reactivities of these metal atom dimers is a first step toward an understanding of the physical and chemical properties of metal atom clusters. Because of their high reactivity, metal atom clusters are widely used for catalytic processes. In addition, larger clusters with a diameter in the nm range (ideally 1–2 nm) exhibit quantum-size effects, which make their use in single-electron devices attractive. In spite of these wide-ranging applications, detailed information about the structures and electronic properties of metal atom clusters is sparse. There are not only experimental difficulties. Quantum chemical calculations become extremely difficult and expensive, even in the case of the metal atom dimers. Multi-reference methods have to be applied and inner-core correlation has to be taken into account. Often DFT methods fail or are not really reliable.

Although clusters are generally more reactive than metal atoms or ideal defect-free surfaces, first results show that there are large differences between clusters that consist of different numbers of atoms. In some cases, the maximum reactivity of an M_n particle (where M denotes a metal atom and $n \geq 1$) seems to be reached at the stage of the metal atom dimer. Thus, gas-phase studies revealed that Rh_2^+ brings about a spontaneous dehydrogenation reaction with CH_4, while Rh^+ ions and Rh_n^+ clusters ($n \geq 3$) do not induce spontaneous reaction [2]. In the same vein, Pt_2^+, but not Pt^+ ions or Pt_n^+ clusters, were found to react with NH_3 to give the dehydrogenation product $[Pt_2NH]^+$ [3].

After a brief description of the matrix-isolation technique, the results which have led to a detailed characterization of Ga_2 and Ti_2 will be reported. Thereafter, the reactions between Ga_2 and H_2 and between Ti_2 and N_2 are discussed. These two model reactions underline impressively the high reactivity of metal atom dimers.

Inorganic Chemistry in Focus II. Edited by G. Meyer, D. Naumann, and L. Wesemann

ISBN: 3-527-30811-3

1.2 Principle and Realization of the Matrix-Isolation Experiment

In the matrix-isolation experiment, the two reactants are isolated in a host material, which generally consists of a frozen inert gas (e.g. argon) to minimize chemical interactions between the host and the isolated reactants (Fig. 1.1). The temperature is kept very low (at a few Kelvin). At these temperatures, even small reaction barriers (of a few kJ mol^{-1}) cannot easily be surmounted (kT=0.08 kJ mol^{-1} at 10 K), if tunnelling processes can be neglected. Therefore, reaction intermediates that cannot survive under other conditions can be generated, trapped, and observed. Indeed, one of the great advantages of the matrix-isolation method is that the reaction intermediates can be retained for several hours or even days and therefore can be identified and characterized at leisure by applying standard laboratory techniques.

The identification and characterization of possible intermediates and reaction products usually relies on spectroscopic methods. Vibrational spectroscopy is certainly the most widely applied method, combining as it does the advantages of high sensitivity and the provision of information that can not only be used to identify the species, but also to determine some important properties such as symmetry and more detailed structural information, force constants, and, in some cases, dissociation energies (see below). To allow for a better analysis of the data, the experiments have to be repeated with as many isotopomers as possible. These isotopomers usually have to be synthesized especially for this purpose. The experimental results are often accompanied by quantum chemical calculations, which allow for a further characterization. Absorption spectroscopy with radiation energy sufficiently high to excite electrons within the species isolated in the matrix provides valuable information about possible photochemistry and may be used to analyze the properties of excited states. Thus, if the spectra are vibrationally resolved, the frequency and important structural information can be obtained for some excited states of the species under investigation. Fluorescence spectroscopy can also be extremely informative, although this technique can only be applied in certain cases. Finally, radicals might be studied by means of EPR spectroscopy (see ref. [1] for more information on possible methods of interrogation).

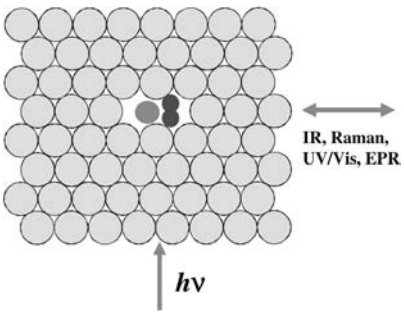

Fig. 1.1 Two reactants are isolated in a defect of the polycrystalline matrix host material. The spontaneous and photolytically induced reactions can be followed by means of spectroscopic methods, such as absorption (vibrational or electronic excitations), emission, or EPR spectroscopy.

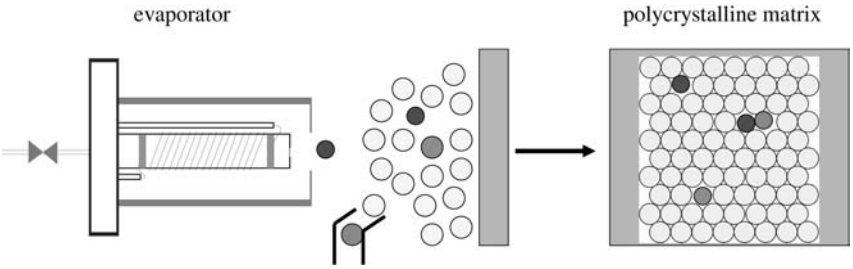

Fig. 1.2 Preparation of a matrix which contains two reactants. One of them is produced in an evaporator, the second is admixed to the matrix gas. The result is a statistical distribution of the two reactants in defect sites of the matrix host.

Fig. 1.2 illustrates the preparation of a matrix in a typical matrix experiment. In the studies discussed herein, one of the reactants is emitted from a metal evaporator. For example, gallium vapor can be generated by resistively heating the metal in a BN cell, or an alumina tube containing a carbon cell, to a temperature of 900–1000 °C. An element like titanium, for which higher temperatures are necessary, may be evaporated by directly heating a pure metal wire (to 1600–1700 °C in the case of titanium). The amount of deposited metal can be monitored with the aid of a microbalance. The other reactant is admixed to the matrix gas. The matrix is deposited onto a metal block (e.g., Cu or Rh-plated Cu) kept at a low temperature (10 K in general), generally by means of a closed-cycle refrigerator. UV/Vis spectra give useful information about the metal atom to metal atom dimer ratio in the matrix.

1.3 Characterization of Metal Atom Dimers

Metal atom dimers in a matrix can be characterized by means of absorption (e.g. UV/Vis), resonance-Raman, and/or fluorescence spectroscopy. In some cases, the resonance-Raman spectra reveal not only the ν(M–M) stretching fundamental, but also several overtones. These overtones can be used to estimate the dissociation energy, which is an important parameter in describing the metal–metal bond. It is also of importance for the understanding of reaction mechanisms, since the metal–metal bond is often ruptured in the course of the reaction. Thus, the energy required for the rupture of the metal–metal bond has to be compensated by the formation of other bonds if the reaction is to proceed spontaneously. In the following, the results obtained for Ti_2 and Ga_2 from matrix-isolation experiments and quantum chemical calculations are discussed. These two metal atom dimers were chosen exemplarily because, as detailed below, they show remarkably high reactivities.

Ti_2 Fig. 1.3 shows the resonance-Raman spectra obtained for Ti_2 measured with the $\lambda = 514.532$ nm line of an Ar^+ ion laser [4]. Some regions of the spectrum are

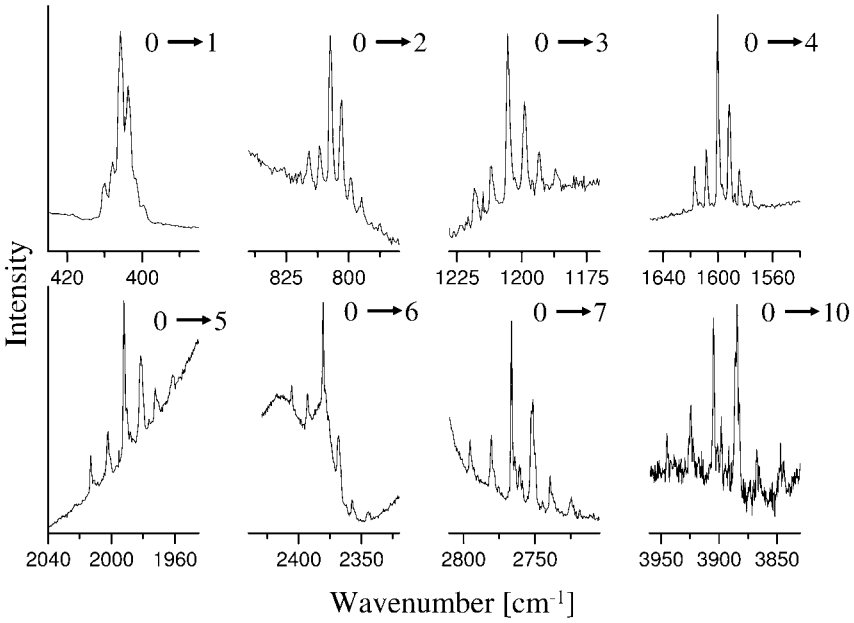

Fig. 1.3 Resonance Raman spectra of Ti_2 isolated in an Ar matrix (measured with the 514.532 nm line of an Ar^+ ion laser).

covered by fluorescence signals, which for the most part belong to Ti atoms. Nevertheless, in the regions free from fluorescence signals, a series of overtones can be measured, which exhibit an isotopic splitting. The results can be used to estimate the dissociation energy on the basis of a LeRoy–Bernstein–Lam analysis [5]. In this analysis, the potential near the dissociation limit is assumed to be a quadrupole-quadrupole-type interaction between two Ti atoms in their ^{3}F electronic ground state. One then interpolates between the formulas derived for the vibrational level energies near the dissociation limit (resulting from a WKB treatment) and those that are closer to the bottom of the potential-energy curve. The analysis yields a dissociation energy (D_e value) of 113.9 kJ mol^{-1} [4].

Additional valuable information is provided by absorption measurements. Fig. 1.4 shows the absorption spectrum of Ti_2 in the region between 4000 and 6500 cm^{-1} [6]. Two series of bands are visible, which can be assigned to excitations into different vibrational levels of the $1\,^3\Pi_u$ and the $1\,^3\Phi_u$ states. The relative intensities of the bands in each series can be used to estimate the difference Δr_e in the bond distances between the excited state and the ground state on the basis of a Franck–Condon analysis. To this end, Morse-type functions were assumed for each state. The analysis resulted in Δr_e values of 9 pm for the $1\,^3\Pi_u \leftarrow {}^3\Delta_g$ and of 10 pm for the $1\,^3\Phi_u \leftarrow {}^3\Delta_g$ transition. Thus, the Ti–Ti bond length is found to increase in both electronically excited states relative to the ground state.

Experimental information was also obtained for the next higher $2\,^3\Pi_u$ and $2\,^3\Phi_u$ states. In these states, the Ti–Ti bond is even longer. Tab. 1.1 includes Δr_e,

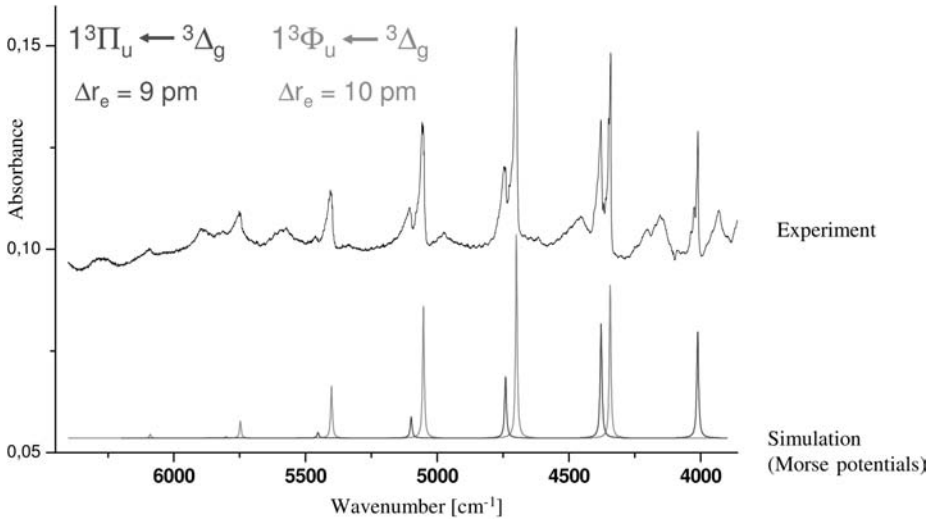

Fig. 1.4 Absorption spectrum of Ti_2 in the region between 4000 and 6500 cm^{-1}. The bands are due to two vibrationally resolved electronic excitations.

Tab. 1.1 Comparison between the experimentally determined and calculated [MRCI (ANO 76432)] relative bond distances Δr_e (in pm), the harmonically corrected frequencies, and the excitation energies T_e (in kJ mol^{-1})

Electronic state	Δr_e		ω_e		T_e	
	exp.	calcd.	exp.	calcd.	exp.	calcd.
$^3\Delta_g$	0	0	407.0	369	0	0
$1\ ^3\Pi_u$	9 ± 2	11.3	371.5	330	48.2	40.5
$1\ ^3\Phi_u$	10 ± 2	12.2	359.5	317	52.1	42.5
$2\ ^3\Pi_u$	13 ± 2	17.4	282.0	259	83.9	71.4
$2\ ^3\Phi_u$	13 ± 4	17.0	288.2	268	99.4	91.7

the harmonic frequencies ω_e, and the excitation energies T_e for all states for which detailed experimental information is available. Tab. 1.1 also compares the experimentally derived values with those predicted by high-level quantum chemical calculations (MRCI method).

Ga_2 Again, resonance-Raman spectroscopy proves to be extremely useful to obtain information about the ground state of the dimer. The resonance-Raman spectrum of Ga_2 is displayed in Fig. 1.5 [7]. The ν(Ga–Ga) stretching fundamental occurs at 176.5 cm^{-1}. Three additional signals in the spectrum can be assigned to the first, second and third overtones. The signals show an isotopic

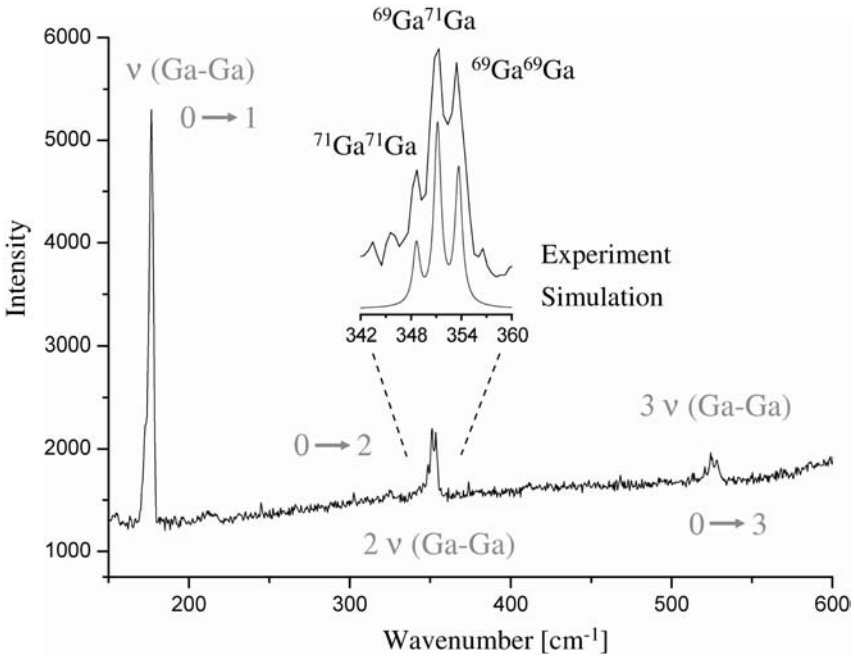

Fig. 1.5 Resonance Raman spectrum of Ga_2, obtained with the 514.532 nm line of an Ar^+ ion laser.

Tab. 1.2 Calculated dimensions (in pm), harmonic vibrational frequencies (in cm^{-1}), and relative energies (in kJ mol^{-1}) of Ga_2 in various electronic states

Ga_2		CASSCF/SVP	MP2/TZVPP	Exp.
$^3\Pi_u$	d(Ga–Ga)	276.3	271.4	
	ω(Ga–Ga)	161	178	175
$^3\Sigma_g^-$	ΔE	7.1	7.8	
	d(Ga–Ga)	251.0	247.1	
	ω(Ga–Ga)	204	222	
$^1\Sigma_g^+$	ΔE	19.0	41.5	
	d(Ga–Ga)	309.3	300.3	
	ω(Ga–Ga)	121	146	
$^1\Pi_u$	ΔE	46.3		
	d(Ga–Ga)	278.1		
	ω(Ga–Ga)	154		
$^1\Delta_g$	ΔE	56.4		
	d(Ga–Ga)	258.7		
	ω(Ga–Ga)	170		

splitting that is in pleasing agreement with the pattern expected for Ga_2 (see inset in Fig. 1.5) in its three isotopic forms $^{69}Ga^{69}Ga$, $^{69}Ga^{71}Ga$, and $^{71}Ga^{71}Ga$. The dissociation energy of Ga_2 can be estimated to be ca. 130 kJ mol^{-1}.

Unfortunately, it has hitherto not been possible to obtain detailed information about excited states of Ga_2 with energies close to the ground state. Calculations indicate that a $^3\Sigma_g^-$ state has an energy which is only ca. 7 kJ mol^{-1} higher than that of the $^3\Pi_u$ ground state. Several singlet states are also predicted to be close by in energy (see Tab. 1.2) [10]. It will be shown below that these excited states play a significant role in relation to the reactivity of Ga_2.

1.4 Reactivity of Metal Atom Dimers and Comparison with the Reactivity of Single Metal Atoms

In the following, two examples are discussed which should underline the strikingly high reactivity of metal atom dimers, namely the reaction of Ga_2 with H_2 and the reaction of Ti_2 with N_2. Both reactions proceed spontaneously with the metal atom dimers in their ground electronic states.

1.4.1 The Reaction Between Ga_2 and H_2

Ga atoms in their electronic ground state (^{2}P) do not react with dihydrogen. A reaction can only be brought about by photoactivation of the Ga atoms ($^2S \leftarrow {}^2P$ excitation), thereby leading to the bent radical GaH_2 [8, 9]. This result is at first glance surprising, since transition metal atoms are known to react spontaneously with H_2 only after one of the d electrons has been excited into an empty p orbital. On this basis, it has been argued that the attractive interaction between the half-filled p orbital and the σ^* orbitals at the dihydrogen initiates the reaction. A correlation diagram shows, however, that the ground state of the $Ga\cdots H_2$ system (with a large separation between Ga and H_2) correlates with an excited state of the product GaH_2. Therefore, the thermal reaction is subject to a massive reconfiguration barrier [10]. In fact, a radical mechanism is favored, which leads first to GaH and H atoms, and these combine in the second step to give the GaH_2 radical. Thus, although the overall reaction is slightly endothermic (by 16 kJ mol^{-1} according to MP2/TZVPP), [10] photolysis is needed for the reaction to take place.

For the reaction between Ga_2 and H_2, one might also assume at first glance a significant barrier, since the reaction is formally spin-forbidden (Ga_2 exhibits a triplet ground electronic state and Ga_2H_2 a singlet one). However, spin-orbit coupling is significant and provides a means by which the system can change its multiplicity from triplet to singlet. The experiments show that Ga_2 reacts spontaneously with H_2 to give the cyclic, D_{2h} symmetric $Ga(\mu\text{-}H)_2Ga$ molecule (see Fig. 1.6) [10]. Calculations indicate that the reaction proceeds via excited states of Ga_2. Thus, in the early stage of the approach between the two reactants, the $^3\Pi_u$ and $^3\Sigma_g^-$ type states

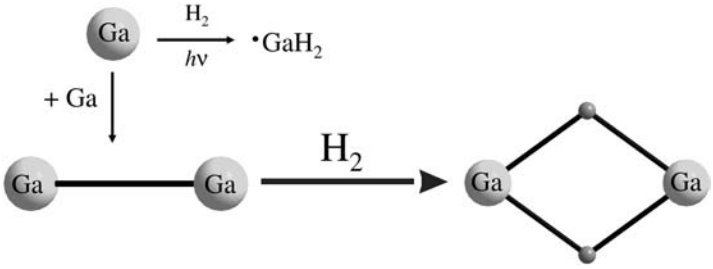

Fig. 1.6 Ga_2 reacts spontaneously with H_2 to give the cyclic, D_{2h} symmetric $Ga(\mu\text{-}H)_2Ga$ ring. Ga atoms react with H_2 only upon photoactivation, the product being the bent radical GaH_2.

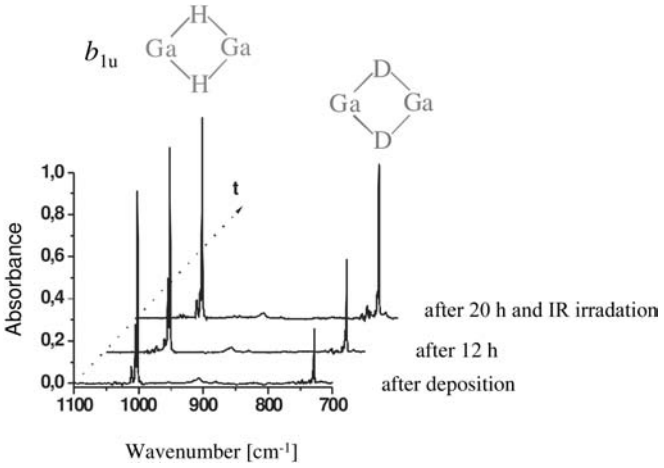

Fig. 1.7 IR spectra taken for an Ar matrix containing Ga_2 and a 1:1 mixture of H_2/D_2.

of Ga_2 mix. At the point of intersystem crossing from triplet to singlet state, a $^1\Delta_g$ type state is adopted. As a consequence, the Ga–Ga distance first shortens from 276 to 255 pm. The relevant excited states have energies which are relatively close to that of the ground state. Therefore, the barrier to reaction is relatively low. The experiments give additional information about the reaction mechanism. Thus, the reaction proceeds spontaneously with H_2, but not with D_2. In the case of D_2, the matrix has to be kept for several hours in the dark or irradiated with IR light to complete the reaction (see Fig. 1.7). This isotopic effect indicates that the barrier to reaction is of the order of the zero-point energy difference between H_2 and D_2, viz. ca. 30 kJ mol^{-1}. This value is slightly lower than the calculated estimate (ca. 50 kJ mol^{-1}). Nevertheless, both experiment and theory agree in that Ga_2 is much more reactive toward H_2 than a single Ga atom.

It is worth mentioning that $Ga(\mu\text{-}H)_2Ga$ can be converted into two other isomeric forms when the molecule is selectively photolyzed (see Fig. 1.8). In both

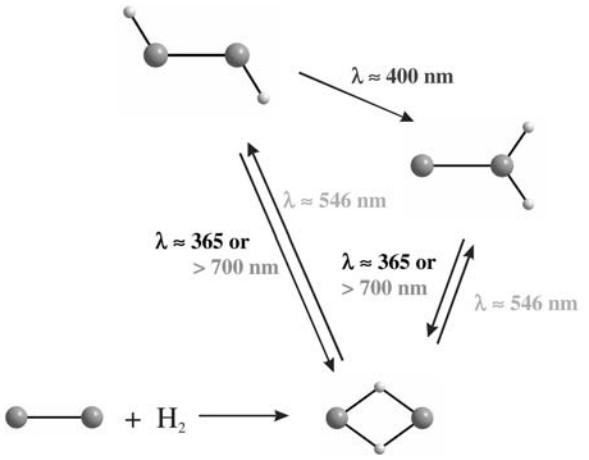

Fig. 1.8 Photoconversion of $Ga(\mu\text{-}H)_2Ga$ into the two isomers HGaGaH and $GaGaH_2$.

of these isomers, direct Ga–Ga bonds exist. One of the isomers is the *trans*-bent species HGa–GaH. Analysis of the spectra obtained for this molecule in combination with quantum chemical calculations clearly shows that the Ga–Ga bond is most adequately described as a relatively weak donor–acceptor interaction between two GaH diatomics. According to quantum chemical calculations, the energy for fragmentation of HGa–GaH into two non-relaxed GaH units with singlet electronic state amounts to no more than 57 kJ mol^{-1} [11]. This again shows that the Ga–Ga bond is weak. At 262.0 pm, the calculated Ga–Ga bond distance is relatively long. Meanwhile, there are structural data (from X-ray diffraction analyses) available for some derivatives Ar′GaGaAr′ (e.g., with Ar′ being 2,6-$Dipp_2C_6H_3$, Dipp = 2,6-$i Pr_2C_6H_3$) [12, 13]. These data confirm the analysis made for HGaGaH. Like HGaGaH, the derivatives exhibit a *trans*-bent structure. The Ga–Ga bond distance in Ar′GaGaAr′ amounts to 262.68(7) pm. The results also indicate that the Ga–Ga bond in the dianion $[HGaGaH]^{2-}$ cannot be adequately described as a triple bond and thus the properties differ to a large extent from those found for HCCH. This is also reflected in the different structures (*trans*-bent in the case of $[HGaGaH]^{2-}$ vs. linear for HCCH). The crystal structures of derivatives $[RGaGaR]^{2-}$ [e.g., R being 2,6-(2,6-$i Pr_2C_6H_3)_2C_6H_3$] [14] were determined and the Ga–Ga distance was found to be short (231.9 pm). However, this short distance does not necessarily imply the presence of a triple bond. An analysis indicates that the Na^+ cations are engaged in the bonding [15, 16]. At the same time, the Na^+ ion interacts with the aromatic rings on the ligands. That the Ga–Ga bond length has to be taken with caution as a criterion for the bond order also becomes evident if the values determined for typical Ga–Ga single bonds are compared. Thus, in $Ga_2[Ga_2I_6]$, the Ga–Ga bond length is 238.7(5) pm [17]. At the other extreme, a value of 254.1(1) pm was determined in the case of $Ga_2(Trip)_4$ (Trip = 2,4,6-$i Pr_3C_6H_2$) [18] and also for $Ga_2[CH(SiMe_3)_2]_4$ [19].

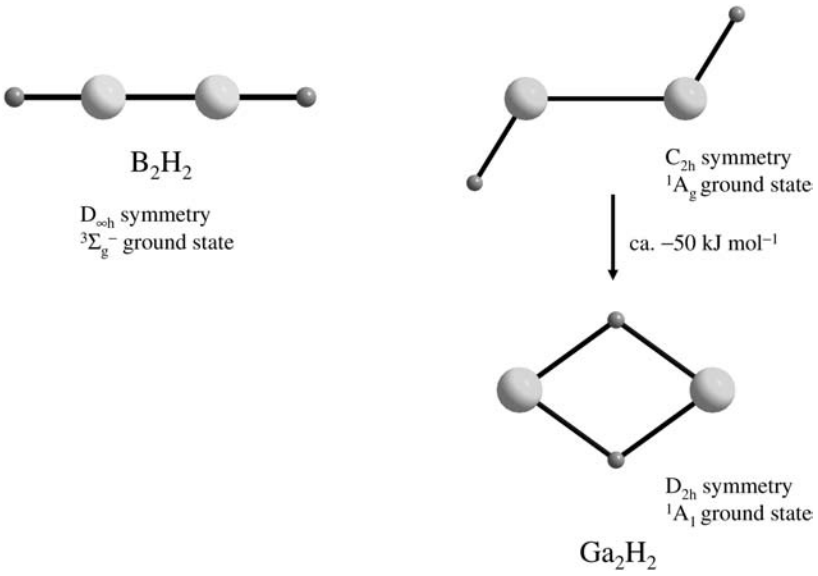

Fig. 1.9 Comparison between the structures of B_2H_2 and its homologue Ga_2H_2.

In contrast to HGaGaH, the lighter homologue HBBH is a linear molecule with a triplet electronic ground state (see Fig. 1.9). The molecule has been characterized in matrix by IR [20] and EPR [21] spectroscopies, and has also been the subject of theoretical work [22]. The results show that, as anticipated, the triplet state arises from the presence of two degenerate π-orbitals, which are each occupied by one electron. The B–B bond is strong (in line with a formal bond order of 2) and the calculated B–B distance amounts to 150.7 pm. Fragmentation of HBBH into two geometrically non-relaxed HB units with singlet electronic states requires ca. 450 kJ mol^{-1} [CCSD(T) estimate] [11]. Nevertheless, the dimerization of the molecule to give B_4H_4 in its tetrahedral global energy minimum structure is predicted to be highly exothermic [ca. –482 kJ mol^{-1} according to CCSD(T) calculations] [23].

Recently, it has been shown that Ga_2 reacts spontaneously not only with H_2, but also with SiH_4 [24]. Interestingly, the product formed in this reaction is HGa(μ-SiH_3)Ga, featuring a terminal Ga–H bond and the SiH_3 group in a bridging position.

1.4.2
The Reaction Between Ti_2 and N_2

According to matrix experiments, Ti atoms in their electronic ground state do not engage in a complex with dinitrogen. Ti_2 dimers, however, undergo spontaneous reaction with N_2. In the course of this reaction, which proceeds without

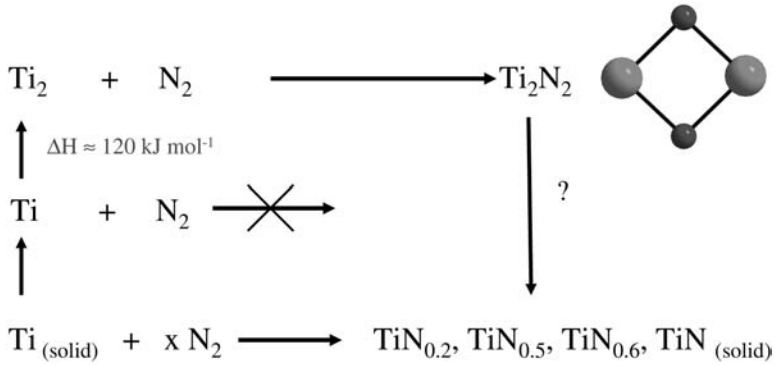

Fig. 1.10 The reaction between Ti_2 and N_2 leads to the cyclic $Ti(\mu\text{-}N)_2Ti$ molecule, which might be an intermediate on the way to solid nitrides of titanium.

a significant barrier, four Ti–N bonds are formed at the expense of the strong NN triple bond, leading to a cyclic $Ti(\mu\text{-}N)_2Ti$ molecule (see Fig. 1.10) [25]. The spectra indicate that the product features no direct N–N interaction. The ground state of $Ti(\mu\text{-}N)_2Ti$ is a singlet state, but a triplet state is of very similar energy. It was possible to detect some vibrationally resolved excitations around 9000 cm^{-1} attributable to this species [25]. This reaction is especially interesting since solid Ti has been shown to react at higher temperatures with molecular nitrogen to first give compounds which contain N atoms dissolved in solid titanium ($TiN_{0.20}$ intercalation compound), with the h.c.p. structure of α-Ti. Finally, with increasing concentration of nitrogen and at ca. 900 °C, a defect NaCl structure is adopted. Thus, in the course of this reaction, the NN bond of dinitrogen has to be ruptured. Ti_2N_2 might be a possible intermediate on the way to these solid phases. A goal of future studies should be the estimation of the reaction enthalpy of Ti_2N_2 formation. This value could then be used to calculate the enthalpy difference between Ti_2N_2 and solid titanium nitride. Solid titanium nitride coatings are of interest as protection layers and as semiconductors.

The isodesmic reaction $2\,TiCl_4+Si_2N_2 \rightarrow 2\,SiCl_4+Ti_2N_2$ can be used to estimate the standard enthalpy of formation for Ti_2N_2. This reaction was calculated to be exothermic by –194 kJ mol^{-1}. First, the enthalpy of formation for Si_2N_2 has to be estimated. The enthalpy for the reaction $2Si(g)+N_2(g) \rightarrow Si_2N_2(g)$ was calculated to be ca. –650 kJ mol^{-1} [26]. With values of +450 kJ mol^{-1} for the standard enthalpy of formation for Si(g) [27], the standard enthalpy of formation of Si_2N_2 amounts to ca. +250 kJ mol^{-1}. With this value, the standard enthalpy of formation of $Ti_2N_2(g)$ can be estimated to be of the order of –49 kJ mol^{-1} (with values of –763.2 and –662.8 kJ mol^{-1} for the standard enthalpies of formation of $TiCl_4$ and $SiCl_4$, respectively [27]). Considering a value of 945.4 kJ mol^{-1} for the standard enthalpy of formation of two single N atoms, this value demonstrates the high affinity of titanium for nitrogen.

It also implies that the reaction between Ti_2(g) (for which the enthalpy of formation is ca. +827 kJ mol^{-1}) and N_2 has to be highly exothermic (standard reaction enthalpy ca. –876 kJ mol^{-1}). The enthalpy of formation of solid TiN was determined to be –337.7 kJ mol^{-1}. Thus, the enthalpy for the reaction $2\,Ti(s)+N_2 \rightarrow 2\,TiN(s)$ amounts to –675.4 kJ mol^{-1}. This value is smaller than the –876 kJ mol^{-1} estimated for the enthalpy of formation of Ti_2N_2(g) from Ti_2(g) and N_2. These considerations do not prove, but support the view that the barrier for the formation of solid TiN from solid Ti and N_2 is caused by the thermal energy required to form "Ti_2" or other small clusters from solid Ti. According to these calculations, Ti_2N_2 could very well be an intermediate on the way to solid titanium nitride.

1.5 Concluding Remarks

The examples discussed herein demonstrate impressively how reactive metal atom dimers are. Electronically excited states with energies close to the ground state are often responsible for these high reactivities (as shown explicitly for the reaction between Ga_2 and H_2) [10]. Therefore, an understanding of the reaction mechanisms requires knowledge of the properties of the ground state and the excited states of these species. A detailed characterization can only be achieved through a combination of experimental and quantum chemical results. However, calculations are extremely difficult and multi-reference methods have to be applied. Inner-core correlation effects have to be rigorously included. As regards experiments, absorption and Raman spectroscopies have been shown to provide useful information on the matrix-isolated species.

The aims of future studies include the characterization of metal atom trimers and other small clusters and the analysis of their reactivity. The clusters can be generated by diffusion of metal atoms or dimers into the matrix upon annealing. Many new fascinating results are expected to emerge from these studies. They might prove to be valuable for possible applications in materials science and catalytic processes.

References

1 See, for example: H.-J. Himmel, A. J. Downs, T. M. Greene, *Chem. Rev.* **2002**, *102*, 4191.

2 Albert, C. Berg, M. Beyer, U. Achatz, S. Joos, G. Niedner-Schatteburg, V. E. Bondybey, *Chem. Phys. Lett.* **1997**, *268*, 235.

3 K. Koszinowksi, D. Schröder, H. Schwarz, *J. Phys. Chem. A* **2003**, *107*, 4999.

4 H.-J. Himmel, A. Bihlmeier, *Chem. Eur. J.* **2004**, *10*, 627.

5 See, for example: R. J. Le Roy, W.-H. Lam, *Chem. Phys. Lett.* **1980**, *71*, 544.

6 O. Hübner, H.-J. Himmel, W. Klopper, L. Manceron, *J. Chem. Phys.*, **2004**, *121*, 7195.

7 H.-J. Himmel, B. Gaertner, *Chem. Eur. J.* **2004**, *10*, 5936. See also a previous report: F. W. Froben, W. Schulze, U. Kloss, *Chem. Phys. Lett.* **1983**, *99*, 500.

8 P. Pullumbi, C. Mijoule, L. Manceron, Y. Bouteiller, *Chem. Phys.* **1994**, *185*, 13.

9 L. B. Knight, Jr., J. J. Banisaukas III, R. Babb, E. R. Davidson, *J. Chem. Phys.* **1996**, *105*, 6607.

10 a) A. Köhn, H.-J. Himmel, B. Gaertner, *Chem. Eur. J.* **2003**, *9*, 3909. b) H.-J. Himmel, L. Manceron, A. J. Downs, P. Pullumbi, *Angew. Chem.* **2002**, *111*, 829; *Angew. Chem. Int. Ed.* **2002**, *41*, 796. c) H.-J. Himmel, C. Manceron, A. J. Downs, P. Pullumbi, *J. Am. Chem. Soc.* **2002**, *124*, 4448.

11 H.-J. Himmel, H. Schnöckel, *Chem. Eur. J.* **2003**, *9*, 748.

12 N. J. Hardman, R. J. Wright, A. D. Phillips, P. P. Power, *Angew. Chem.* **2002**, *114*, 2966.

13 N. J. Hardman, R. J. Wright, A. D. Phillips, P. P. Power, *J. Am. Chem. Soc.* **2003**, *125*, 2667.

14 J. Su, X. W. Li, R. C. Crittendon, G. H. Robinson, *J. Am. Chem. Soc.* **1997**, *119*, 5471.

15 N. Takagi, M. W. Schmidt, S. Nagase, *Organometallics* **2001**, *20*, 1646.

16 H.-J. Himmel, H. Schnöckel, *Chem. Eur. J.* **2002**, *8*, 2397.

17 (a) J. C. Beamish, M. Wilkinson, I. J. Worrall, *Inorg. Chem.* **1978**, *17*, 2026. (b) G. Geriach, W. Hönle, A. Simon, *Z. Anorg. Allg. Chem.* **1982**, *486*, 7.

18 X. He, R. A. Bartlett, M. M. Olmstead, K. Ruhlandt-Senge, R. W. Sturgeon, P. P. Power, *Angew. Chem.* **1993**, *105*, 761.

19 W. Uhl, M. Layh, T. Hildenbrand, *J. Organomet. Chem.* **1989**, *364*, 289.

20 T. J. Tague, Jr., L. Andrews, *J. Am. Chem. Soc.* **1994**, *116*, 4970.

21 L. B. Knight, Jr., K. Kerr, P. K. Miller, C. A. Arrington, *J. Phys. Chem.* **1995**, *99*, 16842.

22 See, for example: (a) J. D. Watts, R. J. Bartlett, *J. Am. Chem. Soc.* **1995**, *117*, 825. (b) P. R. Schreiner, H. F. Schaefer III, P. v. R. Schleyer, *J. Chem. Phys.* **1994**, *101*, 7625.

23 H.-J. Himmel, *Eur. J. Inorg. Chem.* **2003**, 2153.

24 B. Gaertner, H.-J. Himmel, V. A. Macrae, A. J. Downs, T. M. Greene, *Chem. Eur. J.* **2004**, *10*, 3430.

25 H.-J. Himmel, L. Manceron, publication in preparation. This molecule was previously detected in laser ablation experiments: G. P. Kushto, P. F. Souter, G. V. Chertihin, L. Andrews, *J. Chem. Phys.* **1999**, *110*, 9020.

26 BP/TZVPP calculations. The structure calculated for Si_2N_2 was compared to the one calculated previously (G. Maier, H. P. Reisenauer, J. Glatthaar, *Organometallics* **2000**, *19*, 4775). Si_2N_2 was generated and characterized in matrix-isolation experiments.

27 M. W. Chase, Jr., NIST-JANEF Thermochemical Tab.s, 4th Edition, *J. Phys. Chem. Ref. Data, Monograph* **1998**, *9*, 1–1951.